Research Paper

Role of Particle Size in Phagocytosis of Polymeric Microspheres

Julie A. Champion,[1] Amanda Walker,[1] and Samir Mitragotri[1,2]

Purpose. Polymeric microspheres are extensively researched for applications in drug and vaccine delivery. However, upon administration into the body, microspheres are primarily cleared via phagocytosis by macrophages. Although numerous studies have reported on the biochemical pathways of phagocytosis, relatively little is known about the dependence of phagocytosis on particle size. Here, we investigate the previously unexplained dependence of phagocytosis on particle size.

Methods. Rat alveolar macrophages and IgG-opsonized and non-opsonized polystyrene microspheres were used as model macrophages and drug delivery particles. Phagocytosis, attachment and internalization were measured by flow cytometry and time-lapse video microscopy.

Results. Particles possessing diameters of 2–3 μm exhibited maximal phagocytosis and attachment. Rate of internalization, however, was not affected significantly by particle size. Maximal attachment of 2–3 μm microspheres is hypothesized to originate from the characteristic features of membrane ruffles in macrophages. Elimination of ruffles via osmotic swelling nearly eliminated the peculiar size-dependence of phagocytosis. A simple mathematical model is presented to describe the dependence of phagocytosis on particle size.

Conclusions. The dependence of phagocytosis on particle size originated primarily from the attachment step. These results reveal the importance of controlling drug delivery particle size distribution and selecting the size appropriate for avoiding or encouraging phagocytosis.

KEY WORDS: drug delivery; macrophage; microsphere; phagocytosis; size.

INTRODUCTION

Polymeric microspheres have found numerous applications in drug delivery, vaccination, personal care and medical diagnostics (1–3). Microspheres provide an effective means of protecting, releasing and potentially targeting drugs for various biomedical applications. Drug-carrying microspheres have been administered in animals and humans via intravascular (4), inhalation (5), nasal (6), subcutaneous (7) and other routes. Regardless of the route of administration, microspheres are eventually cleared from the body by phagocytosis, which is one of the body's innate modes of defense against invading pathogens and other non-indigenous particulate matter (8). Macrophages, the body's phagocytic cells, bind particles through a receptor mediated process and internalize them by actin-driven engulfment (9). Though this process is undesired for most drug delivery microspheres, there are some cases, such as vaccines, when efficient targeting to macrophages is required (10). Regardless of whether phagocytosis of microspheres is to be avoided or sought, understanding of the relationships between particle properties and phagocytic uptake is crucial.

Phagocytosis by professional phagocytes has been a topic of extensive research over the last several decades (9, 11–14). Most prominently, studies have elucidated the role of Fc receptors $\left(Fc_{\gamma}RI, Fc_{\gamma}RIIA\right)$ in activating Arp2/3 dependent actin polymerization via several intermediate steps ultimately leading to phagosome formation (15). Studies have also reported on phagocytosis via complement (CR1, CR3 and CR4) and scavenger (SR-AI/II, SR-BI and CD36, among others) receptors (9, 11, 16, 17). While the biochemical pathways of phagocytosis have been relatively well studied, the biophysical aspects of phagocytosis, such as the role of particle properties, have been far less studied. It has been established that particle parameters such as size, shape, surface chemistry and mechanical properties influence phagocytosis (18–20). Among these, the role of surface chemistry is perhaps best studied. Modification of particle surfaces with polyethylene glycol and poloxamine is routinely used to reduce phagocytosis by postponing opsonization, or adsorption of proteins which increase phagocytosis (21). However, an in depth understanding of the role of physical parameters and the biophysical origins of these roles is still emerging.

Several studies have been conducted to define the role of size in phagocytosis (22–27). Tabata and Ikada studied phagocytosis of polystyrene microspheres (0.5–4.6 μm) by mouse peritoneal macrophages and reported that maximal phagocytosis was observed for an intermediate particle size (1.7 μm) (23). Similar conclusions were drawn by Rudt *et al.* for human blood granulocytes via indirect measurements of

[1] Department of Chemical Engineering, University of California, Santa Barbara, California 93106, USA.
[2] To whom correspondence should be addressed. (e-mail: samir@engineering.ucsb.edu)

phagocytosis of particles ranging in diameter from 85 nm to 3.2 μm (26). Simon studied the uptake of 0.5–8 μm polystyrene microspheres by human blood neutrophils and leukocytes and reported that phagocytosis decreased with increasing particle size (24). Theoretical work has also been performed to understand the dependence of phagocytosis on particle size (27). These studies predicted that phagocytosis should increase with particle size for hydrophobic particles and decrease for hydrophilic particles. Clearly, the precise dependence of phagocytosis on particle size and its mechanistic origin remain ambiguous. To elucidate previous unexplained or inconsistent results, we separately assess the two steps of phagocytosis, attachment and internalization. Herein, using rat alveolar macrophages as model macrophages and polystyrene particles (1–6 μm) as model microspheres, we report on the dependence of phagocytosis on size and postulate on its mechanistic origin.

MATERIALS AND METHODS

Particles

Green fluorescent non-functionalized polystyrene particles with diameters of 0.93±0.1, 1.87±0.012, 2.3±0.11, 2.98± 0.083, 4.3±0.14, 5.71±0.23 and 9.008±1.28 μm were used as test particles (Polysciences, Warrington, PA). In experiments with "non-opsonized" particles, the particles were used as purchased with no modification. For experiments with "IgG-opsonized" particles, rabbit IgG (Sigma Chemicals, St. Louis, MO) was passively adsorbed onto the polystyrene particles. Particles were taken directly as purchased and incubated in 0.5 ml of 0.25 mg/ml rabbit IgG in phosphate buffered saline (PBS) for 30 minutes at 37°C to achieve opsonization. In the case of larger, less concentrated particles, excess water was removed by centrifugation to reduce the particle volume to 0.1 ml prior to IgG incubation. The particles were washed twice by centrifugation with PBS to remove unbound IgG. Opsonization was verified with fluorescence microscopy using fluorescently tagged IgG (Molecular Probes, Eugene, OR) and by measuring the zeta potential (data not shown). Unmodified particles were negatively charged (zeta potential on the order of −60 mV) while IgG-opsonized particles were neutral (zeta potential ~0 mV). Non-opsonized particles are capable of adsorbing proteins from heat-inactivated fetal bovine serum in the cell media, the primary component being albumin, through hydrophobic interactions upon addition of the particles to cells in supplemented media.

Cells

Continuous alveolar rat macrophage cells NR8383 (American Type Culture Collection (ATCC), Manassas, VA), murine peritoneal macrophages J774 (generous gift of Duane Sears), and human spleen macrophages (ATCC) were used as model macrophages (28). Alveolar and peritoneal cells were cultured in F-12K media (ATCC) and spleen cells were cultured in Iscove's modified Dulbecco Eagle media (ATCC). All media was supplemented with 10% fetal bovine serum and 1% penicillin/streptomycin (Sigma Chemicals). Cells were grown under standard culture conditions (37°C, 5% CO_2, humidified). In overall phagocytosis and attachment assays, both attached and floating cells were sampled since these cell types are not purely adherent cell lines.

Overall Phagocytosis Assay

Supplemented cell medium was replaced with a fresh lot 24 hours prior to the experiment. Cells were seeded in 12 well plates at a concentration of 2×10^5 cell/ml and were allowed to adhere for two hours. In all cases a red fluorescent dye, 55 μM FM4–64 (Molecular Probes, Eugene, OR) was added to the culture medium to stain the cells for identification in flow cytometry. Particles were added to the cells at concentrations ranging from 3 to 1500 particles/cell and incubated for one hour at 37°C, 5% CO_2, humidified. Cells were then scraped from the wells, washed three times with cold PBS to remove unattached particles and analyzed using flow cytometry.

Attachment

Cells were seeded and stained (swollen, if appropriate) using procedures identical to those described above. For swollen cell experiments, media was diluted with water slowly over two hours to a final concentration of 10% media and 2×10^5 cell/ml. The cells were allowed to equilibrate and reattach for two additional hours at 37°C. After ensuring adhesion, the cells were cooled to 4°C. Particles were added to the cells at concentrations ranging from 3 to 1500 particles/cell and allowed to incubate for one hour at 4°C. Cells were then scraped from the wells and washed three times with cold PBS to remove unattached particles and analyzed using flow cytometry.

Attachment of particles to cells was quantified in terms of a Langmuir equilibrium constant defined as $K = \frac{\theta}{(1-\theta)*[P]}$. Where θ is the fraction of cell area occupied by attached particles and [P] is the concentration of unbound particles. Since a large excess of particles were used during attachment (10–300 particles still in suspension for every attached particle), concentration of unbound particles was assumed to remain constant throughout the incubation period. Attachment equilibrium was reached within 15 minutes of incubation and concentration of membrane-bound particles remained constant throughout the rest of the incubation period (data not shown). The definition of K assumes that attachment is a linear process with respect to unbound particle concentration; therefore K is independent of unbound particle concentration. This assumption was experimentally verified by measuring K at various particle/cell ratios (from 3 to 1500) for selected particles. K values were indeed independent of unbound particle concentration over a wide range (data not shown). It should be noted, however, that even at the highest concentration used, attached particles occupied less than 9% of surface area. It is possible that under extremely high particle concentrations (well beyond the range used in this study) where a majority fraction of membrane area is occupied by the particles, K may decrease.

Flow Cytometry

The number of particles attached to and phagocytosed by the cells was assessed using flow cytometry (Partec PAS III

automated flow cytometer with a 100 mW argon laser with a wavelength of 488 nm, Munster, Germany). Cells were identified from free particles by their forward scatter, side scatter and red fluorescence originating from FM4–64. The number of particles associated with cells was determined by processing the green fluorescence of cells with WinMDI software using methods described by Steinkamp (29). Specifically, since the fluorescence of the particles is additive, the total green fluorescence of a cell can be resolved to determine the number of particles associated with that cell. Cell populations with different numbers of particles could be clearly identified by separate peaks in histograms of green fluorescence data (data not shown). The number of cells in each peak was counted and the distribution was averaged to obtain an average number of particles per cell for both attachment and overall phagocytosis. At least 3000 cells were counted for each sample.

Scanning Electron Microscopy

Scanning electron microscopy (SEM) was used to visualize membrane ruffles on macrophages. After one hour of cell attachment to glass coverslips at 37°C, cells were fixed with 2.5% gluteraldehyde. Cells were washed with increasing concentrations of ethanol (up to 100%), vacuum dried and coated with palladium (Hummer 6.2 Sputtering System, Anatech Ltd., Union City, CA). Cells were imaged with the Sirion 400 SEM (FEI Company, Hillsboro, OR) at an acceleration voltage of 2 kV.

Environmental Scanning Electron Microscopy

Environmental scanning electron microscopy (ESEM) was used to measure the ruffled features on macrophage surfaces. Cells were prepared as for SEM but they were washed only with water and not dried, to best retain their original volume. Cells were imaged with an XL30 ESEM (FEI Company) at an acceleration voltage of 5 kV. Images were manually inspected for membrane structures (41 cells) and Metamorph® software was used to estimate the distance between ruffles, L, and the ruffle height, h.

Time-Lapse Video Microscopy

Cells (2×10^5 cells/ml) were allowed to attach in dishes lined with coverslip glass in F-12 K media supplemented with 10% FBS and 25 mM HEPES (Sigma Chemicals). The dishes were placed on an Axiovert 25 microscope (Carl Zeiss Inc., Thornwood, NY) at 100X with phase contrast filters and equipped with Bioptechs Delta T Controlled Culture Dish System® (Bioptechs Inc., Butler, PA) to keep the cells at 37°C. Particles (1 particle per cell) were added to the dishes and bright-field images were collected every 30 seconds by a CoolSNAPHQ CCD camera (Roper Scientific, Tucson, AZ) connected to Metamorph® software. Observed cells were randomly chosen from the entire population thus discounting potential bias due to heterogeneity in macrophage size. Images were condensed into movies and analyzed manually for phagocytic events. Successful phagocytosis exhibited membrane ruffling at the site of attachment, blurring the crisp boundary of the membrane, and subsequent reforming of the membrane boundary after internalization. Additionally, cells were watched for one hour after internalization to verify internalization by particle location on/in the cell. Internalization velocity was calculated as the total distance traveled by macrophage membrane to complete phagocytosis divided by the time required to complete phagocytosis. This method of visual scoring of internalization was validated for IgG-opsonized particles using Alexa Fluor monkey anti-rabbit secondary fluorescent antibody that bound to the rabbit IgG on particles only when they were not internalized (Molecular Probes). Internalization was analyzed based on internalization of one attached particle by a single cell.

RESULTS AND DISCUSSION

Dependence of Phagocytosis on Particle Size

Phagocytosis of microspheres was studied for non-opsonized and IgG-opsonized polystyrene microspheres with diameters ranging from 1 to 6 μm. The number of particles internalized in an hour exhibited an obvious dependence on particle size (Fig. 1). Particles with diameters between 2–3 μm were phagocytosed more readily than both smaller and larger particles. This observation is qualitatively consistent with some of the literature reports (22, 25, 26, 30). Since the receptors involved in phagocytosis of IgG-opsonized and non-opsonized particles are likely to be different (Fc receptors specifically bind IgG-opsonized particles and scavenger receptors non-specifically bind non-opsonized particles (17, 31), the existence of a peak for both particles establishes the generality of the result.
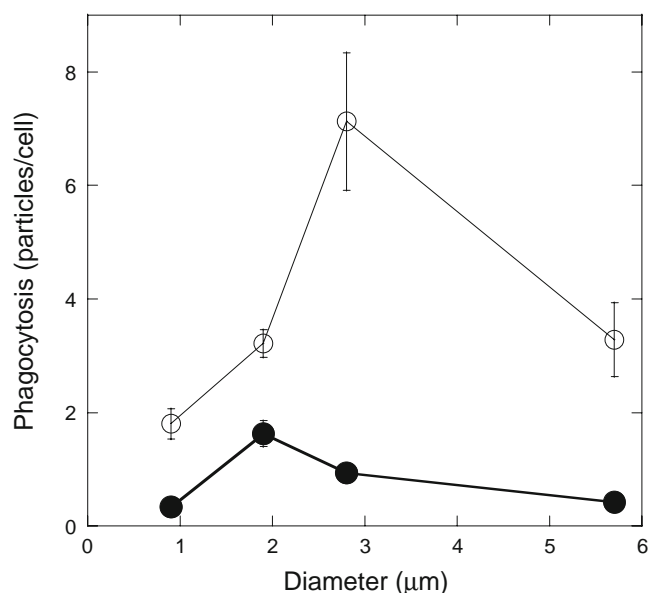

Fig. 1. Overall phagocytosis uptake, combined attachment and internalization, for IgG-opsonized (open circles) and non-opsonized (closed circles) microspheres by rat alveolar macrophages ($n \geq 3$, error bars show one standard deviation).
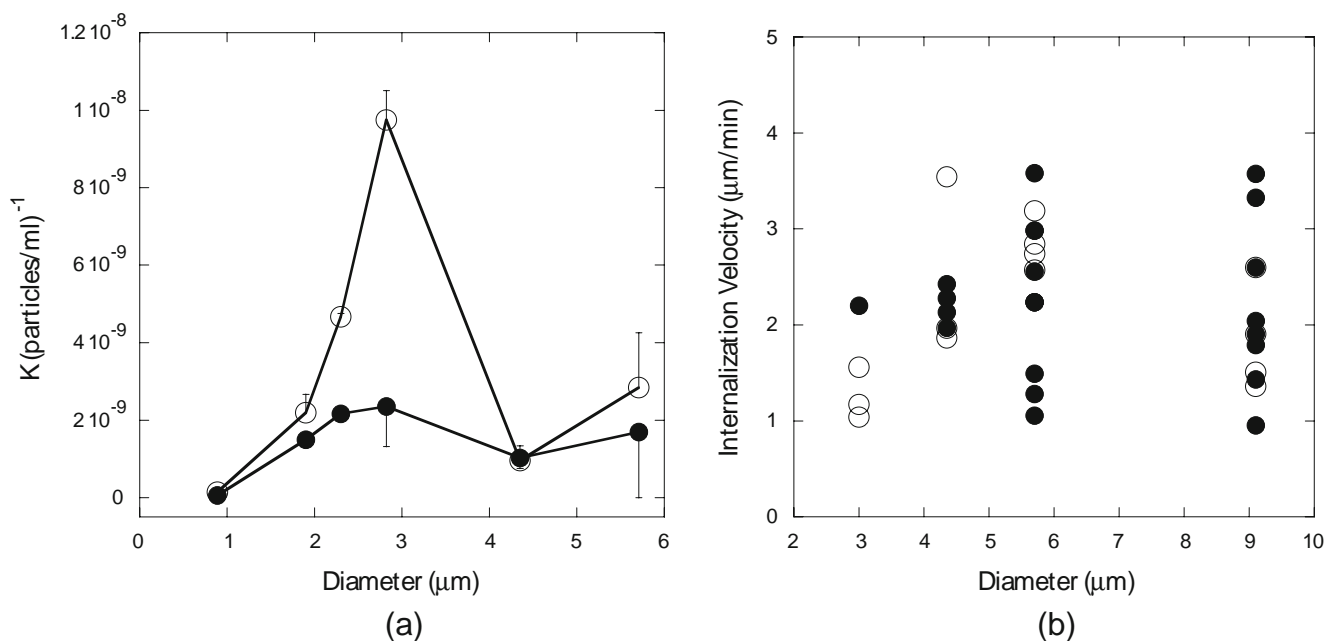
Fig. 2. (a) K values for attachment of IgG-opsonized (open circles) and non-opsonized (closed circles) particles by rat alveolar macrophages. K exhibits a peak for particles with diameters of 2–3 μm, $p<0.00007$ ($n\geq3$, error bars show one standard deviation). (b) Internalization velocities for internalization of IgG-opsonized (open circles) and non-opsonized (closed circles) particles by rat alveolar macrophages. Internalization velocity is not significantly affected by particle size, $p>0.15$ comparing largest and smallest particles.

Role of Particle Size in Attachment

The process of phagocytosis can be divided into two distinct steps, attachment and internalization. We assessed whether the size dependence in Fig. 1 originates from one or both of these steps. Attachment was quantified in terms of a Langmuir equilibrium constant, $K,$ after incubation at 4°C, at which particles cannot be internalized. As expected, IgG-opsonized particles exhibited higher values of K compared to non-opsonized particles. However, the value of K for both types of particles exhibited a clear maximum at a diameter between 2 and 3 μm (Fig. 2a). Opsonization affects the particle charge, hydrophobicity and type of cell receptor to which the particle binds. These major changes, however, did not disrupt the observed size trend. We, therefore, expect that less hydrophobic particles made of drug delivery polymers such as poly(lactide-co-glycolide) will also behave similarly in terms of size-dependence. The location of the peaks in K coincides with the locations of peaks for overall phagocytosis in Fig. 1.

Role of Particle Size in Internalization

To assess whether the process of internalization makes any contribution towards the size dependence of phagocytosis, we monitored internalization of individual particles following attachment using time-lapse video microscopy. Flow cytometry was not used for internalization experiments because actual internalization velocity cannot be measured with this method. Unlike attachment, the speed of internalization (total distance traveled by macrophage membrane to complete phagocytosis divided by the time required to complete phagocytosis) did not exhibit a strong dependence on particle size over a wide range of particle sizes (3–9 μm)

for either type of particles (Fig. 2b). The lack of dependence of internalization velocity on opsonization suggests that Fc and scavenger receptors are equally capable of activating pathways that initiate internalization and on comparable time scales. Most importantly, the results in Figs. 1 and 2 establish that the dependence of phagocytosis on particle size originates from the attachment step.
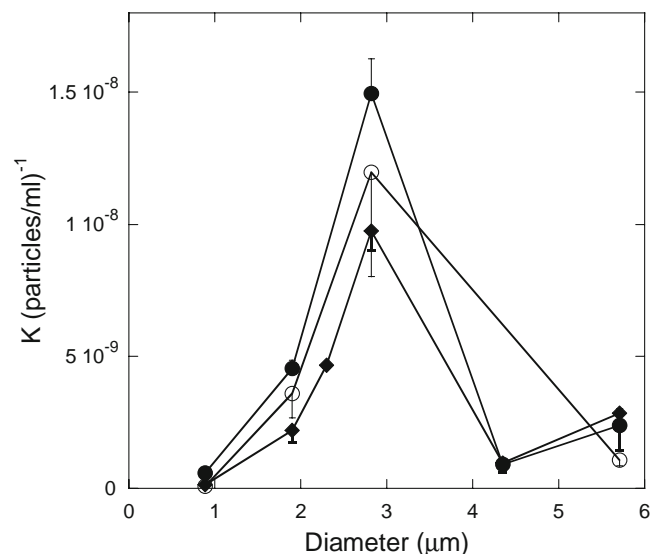

Fig. 3. Comparison of K values for attachment of IgG-opsonized particles by rat alveolar (closed diamonds), murine peritoneal (closed circles) and human spleen (open circles) macrophages. Each macrophage type exhibits a peak in K values around 3 μm diameters, $p< 0.02$ for each type ($n\geq3$, error bars show one standard deviation).

Origins of Size-Specificity of Particle Attachment

Prior to investigating the origin of the peculiar size dependence of particle attachment, we confirmed the generality of the results by measuring attachment of IgG-opsonized polystyrene microspheres to two additional macrophage populations, mouse peritoneal macrophages and human spleen macrophages (Fig. 3). Though the magnitude of attachment varied for the different cell types, a maximum in attachment for 3 μm IgG-opsonized microspheres was consistently observed for all macrophages. Mouse peritoneal macrophages are adherent cells while human spleen macrophages form floating clusters and rat alveolar macrophages have both adherent and floating populations. Although the settling times for all particles are greater than the one hour incubation time, interactions between particles and adherent cells may be more intimate due to settling of particles directly onto the membrane. Interactions between floating cells and particles are more like random collisions and may be weaker. Even more dramatic would be flow conditions where interactions between cells and particles are disrupted by flow. Interestingly, the size trends for both adherent and floating cells are the same, though the magnitudes of attachment are different. This implies that the effect of particle size on attachment is the same among not only different cell types but also potentially among different administration routes where particles are subjected to flow (intravascular injection), Brownian motion (subcutaneous or intramuscular injection), or settling (inhalation).
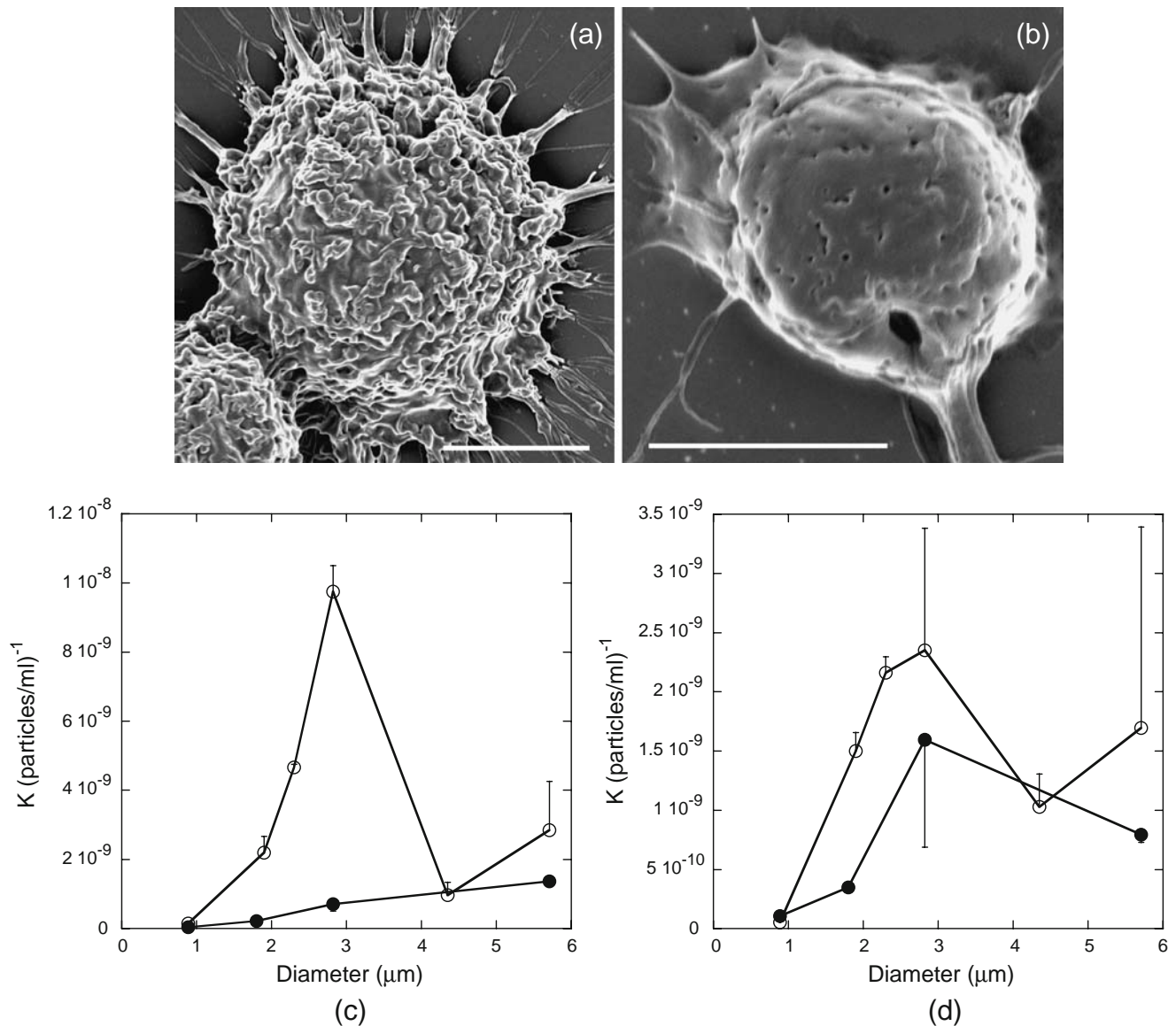

Fig. 4. (a) Scanning electron micrograph of alveolar macrophage displaying a ruffled membrane. Scale bar=5 μm. (b) Scanning electron micrograph of osmotically swollen alveolar macrophage with smooth membrane surface. Scale bar=5 μm. (c) K values for attachment of IgG-opsonized particles by normal (open circles) and swollen (closed circles) rat alveolar macrophages. K values for swollen cells decreased significantly for particles with diameters of 2–3 μm, $p<0.0006$ ($n \geq 3$, error bars show one standard deviation). (d) K values for attachment of non-opsonized particles by normal (open circles) and swollen (closed circles) rat alveolar macrophages. K values for swollen cells decreased significantly for particles with diameters of ~2 μm, $p<0.000002$ ($n \geq 3$, error bars show one standard deviation).

Consistent occurrence of a maximum is surprising considering that macrophages from different species and tissues differ widely in their properties, including size (cell diameter: 5 μm spleen, 10 μm peritoneal, and 15 μm alveolar) (32). One property that is conserved amongst macrophages is a loose, ruffled membrane surface (Fig. 4a) (33). Membrane ruffles are dynamic structures formed by actin filaments and are controlled by complex biochemical pathways, many of which also play important roles in actin-dependent internalization during phagocytosis (9,34,35). We hypothesized that membrane ruffles are responsible for the unusual size dependence of phagocytosis. To assess this hypothesis, rat alveolar macrophages were osmotically swollen to eliminate ruffles (Fig. 4b). Swollen macrophages were then incubated with particles at 4°C. Without the ruffled membrane topography, macrophages did not display the characteristic peak in particle attachment (Fig. 4c, d). Swelling did not result in a general decrease of attachment of all sizes, but instead had the most profound impact on attachment of 2–3 μm particles.

Based on the data in Fig. 4a–d, we postulate that the characteristic peak in size dependence of phagocytosis may originate from the features of membrane ruffles. Interactions of particles with rough surfaces have been previously studied, although in different contexts. Such interactions are typically described using Derjaguin–Landau–Verwey–Overbeek (DLVO) theory (36). Interaction energies of particles with membranes are influenced by size and geometry of both the particles and membrane. Recently, simulations have also been performed to investigate the effect of surface roughness on particle–surface DLVO interactions (37).

Application of DLVO theory to quantitatively predict particle-membrane adhesion based on geometric properties is challenging. As a first step, we postulate that the ruffles impart characteristic local curvature to the membrane and increase contact area between the particle and the macrophage membrane. Thus, microspheres of a certain intermediate size are able to make better contact with the membrane than smaller or larger particles (Fig. 5a). To validate this hypothesis, we modeled ruffles as hemi-spherical membrane protrusions with height, h on a flat membrane with a distance of L between them (Fig. 5b). For the sake of simplicity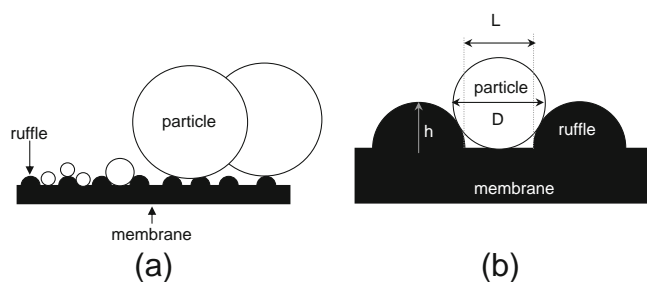, we assumed that both particles and cell membrane are non-flexible. It can be immediately seen from Fig. 5a that the contact area of a particle of diameter D with the membrane depends on the relative magnitudes of h, L, and D. Extremely small particles ($D << L$) will be able to make one contact with the membrane if they contact the protrusion or the flat part of the membrane. In some cases they may attach where the protrusion meets the flat membrane and make two contacts. Extremely large particles ($D >> L$) will also have either one or two contacts depending on whether they attach on the top of a single protrusion or on two protrusions. Intermediate sized particles ($D \sim L$), however, will be able to establish three contact points if they adhere in between the protrusions (Fig. 5b). Mathematically, the particle diameter that maximizes the number of contact points is given by:

$$D_{max} = \frac{L^2 + h^2}{2h}$$

Using Environmental Scanning Electron Microscopy of alveolar macrophages, we measured L and h. From these measurements, $L = 1.9 \pm 0.55 \ \mu m$ and $h = 1 \pm 0.25 \ \mu m$, we estimate $D_{max} = 2.3 \ \mu m$, which compared well to experimentally observed values (Figs. 1, 2a).

CONCLUSIONS

The work presented here significantly enhances the understanding of an important aspect of phagocytosis, size dependence, by separately and directly assessing attachment and internalization of polymeric particles. It shows that the size-dependence of phagocytosis originates from the attachment step and not internalization. The work also puts forth a new hypothesis for the origin of size-dependence of phagocytosis, that the characteristic features of membrane ruffles are responsible for particles size recognition. This conclusion has several implications. First, as a component of innate immunity, macrophages must recognize the most generic features of foreign targets. Through an array of phagocytic surface receptors, macrophages recognize a broad range of foreign molecules on targets. However, the results presented here show that macrophages recognize an even more generic feature, target size. This is a remarkable example of biology creating a physical structure imperative to its function. Second, the data show that size recognition is consistently observed for different macrophage receptors and more surprisingly, for macrophages from three different tissues and species. Conservation of both recognition ability and the size range of recognition (2–3 μm in diameter) could suggest a deeper role for size recognition in biology. Interestingly, 1–4 μm represents the most common size of air-borne and water-borne bacterial pathogens (38,39). Given that pathogen clearance is a primary function of macrophages, it is possible that the highly conserved recognition of 2–3 μm particles plays an important role in pathogen clearance.

The results presented here also have significant implications for drug delivery. Phagocytosis represents the primary mode of particle clearance *in vivo*. While certain applications such as subcutaneous depot injections necessitate reduced phagocytosis for sustained release, others, such as vaccination, require enhanced phagocytosis. Likewise, drug delivery particles can be administered by several methods, such as inhalation, intravascular, subcutaneous or intramuscular in-

Fig. 5. (a) Schematic of membrane ruffles (black) and attached particles (white). Small ($D << L$, left) and large particles ($D >> L$, right) can make 1 or 2 contacts with the membrane. Mid-sized particles ($D \sim L$, center) can make up to 3 contacts. (b) Schematic of ruffle and particle length scales used to calculate the particle diameter capable of making the most membrane contact (h = height of ruffles, L = distance between ruffles and D = particle diameter).

jection. In each particles will interact with different types of macrophages in different flow environments. Accordingly, fundamental and quantitative understanding of phagocytosis holds an important place in drug delivery. Microspheres with diameters between 1–4 μm are commonly used in drug delivery experiments, hence the results presented provide direct knowledge about the implications of size in phagocytosis. Such knowledge is important in selecting appropriate particle size and maintaining a controlled size distribution since the dependence of phagocytosis on size is high in certain ranges (28-fold difference between attachment of particles with diameters of 2.8 and 4.3 μm).

ACKNOWLEDGEMENTS

REFERENCES

1. D. A. LaVan, D. M. Lynn, and R. Langer. Moving smaller in drug discovery and delivery. *Nat. Rev. Drug Discov.* **1**:77–84 (2002).
2. J. Hanes, M. Chiba, and R. Langer. Polymer microspheres for vaccine delivery. *Pharm. Biotechnol.* **6**:389–412 (1995).
3. V. R. Sinha, and A. Trehan. Biodegradable microspheres for protein delivery. *J. Control. Release.* **90**:261–280 (2003).
4. C. X. Song, V. Labhasetwar, X. M. Cui, T. Underwood, and R. J. Levy. Arterial uptake of biodegradable nanoparticles for intravascular local drug delivery: Results with an acute dog model. *J. Control. Release.* **54**:201–211 (1998).
5. M. Sakagami, and P. R. Byron. Respirable microspheres for inhalation: The potential of manipulating pulmonary disposition for improved therapeutic efficacy. *Clin. Pharmacokinet.* **44**:263–277 (2005).
6. Y. Li, H. L. Jiang, K. J. Zhu, J. H. Liu, and Y. L. Hao. Preparation, characterization and nasal delivery of alpha-cobrotoxin-loaded poly(lactide-co-glycolide)/polyanhydride microspheres. *J. Control. Release.* **108**:10–20 (2005).
7. Y. Yamaguchi, M. Takenaga, A. Kitagawa, Y. Ogawa, Y. Mizushima, and R. Igarashi. Insulin-loaded biodegradable PLGA microcapsules: Initial burst release controlled by hydrophilic additives. *J. Control. Release.* **81**:235–249 (2002).
8. S. H. Djaldetti, M. Bergman, R. Djaldetti, and H. Bessler. Phagocytosis—the mighty weapon of the silent warriors. *Microsc. Res. Tech.* **57**:421–431 (2002).
9. A. Aderem, and D. M. Underhill. Mechanisms of phagocytosis in macrophages. *Annu. Rev. Immunol.* **17**:593–623 (1999).
10. S. D. Xiang, A. Scholzen, G. Minigo, C. David, V. Apostolopoulos, P. L. Mottram, and M. Plebanski. Pathogen recognition and development of particulate vaccines: Does size matter? *Methods.* **40**:1–9 (2006).
11. L. Peiser, S. Mukhopadhyay, and S. Gordon. Scavenger receptors in innate immunity. *Curr. Opin. Immunol.* **14**:123–128 (2002).
12. S. P. Hart, J. R. Smith, and I. Dransfield. Phagocytosis of opsonized apoptotic cells: roles for 'old-fashioned' receptors for antibody and complement. *Clin. Exp. Immunol.* **135**:181–185 (2004).
13. S. Greenberg, and S. Grinstein. Phagocytosis and innate immunity. *Curr. Opin. Immunol.* **14**:136–145 (2002).
14. L. -A. H. Allen, and A. Aderem. Mechanisms of phagocytosis. *Curr. Opin. Immunol.* **8**:36–40 (1996).
15. R. May, E. Caron, A. Hall, and L. M. Machesky. Involvement of the Arp2/3 complex in phagocytosis mediated by FcgammaR or CR3. *Nat. Cell Biol.* 2:246–248 (2000).
16. G. Kaplan. Differences in the mode of phagocytosis with Fc and C3 receptors in macrophages. *Scand. J. Immunol.* **6**:797–807 (1977).
17. L. Kobzik. Lung macrophage uptake of unopsonized environmental particulates—role of scavenger-type receptors. *J. Immunol.* **155**:367–376 (1995).
18. K. A. Beningo, and Y. L. Wang. Fc-receptor-mediated phagocytosis is regulated by mechanical properties of the target. *J. Cell Sci.* **115**:849–856 (2002).
19. J. A. Champion, and S. Mitragotri. Role of target geometry in phagocytosis. *Proc. Natl. Acad. Sci. U. S. A.* **103**:4930–4934 (2006).
20. F. L. Ahsan, I. P. Rivas, M. A. Khan, and A. I. T. Suarez. Targeting to macrophages: Role of physicochemical properties of particulate carriers—liposomes and microspheres—on the phagocytosis by macrophages. *J. Control. Release.* **79**:29–40 (2002).
21. D. E. Owens III, and N. A. Peppas. Opsonization, biodistribution, and pharmacokinetics of polymeric nanoparticles. *Int. J. Pharm.* **307**:93–102 (2006).
22. H. Kawaguchi, N. Koiwai, Y. Ohtsuka, M. Miyamoto, and S. Sasakawa. Phagocytosis of latex-particles by leukocytes .1. Dependence of phagocytosis on the size and surface-potential of particles. *Biomaterials.* **7**:61–66 (1986).
23. Y. Tabata, and Y. Ikada. Effect of the size and surface-charge of polymer microspheres on their phagocytosis by macrophage. *Biomaterials.* **9**:356–362 (1988).
24. S. I. Simon, and G. W. Schmidschonbein. Biophysical aspects of microsphere engulfment by human-neutrophils. *Biophys. J.* **53**:163–173 (1988).
25. Y. Tabata, and Y. Ikada. Phagocytosis of polymer microspheres by macrophages. *Adv. Polym. Sci.* **94**:107–141 (1990).
26. S. Rudt, and R. H. Muller. *In vitro* phagocytosis assay of nano- and microparticles by chemiluminescence III Uptake of differently sized surface-modified particles, and its correlation to particle properties and *in vivo* distribution. *Eur. J. Pharm. Sci.* **1**:31–39 (1993).
27. H. M. Chen, R. Langer, and D. A. Edwards. A film tension theory of phagocytosis. *J. Colloid Interface Sci.* **190**:118–133 (1997).
28. R. J. Helmke, V. F. German, and J. A. Mangos. A continuous alveolar macrophage cell-line—comparisons with freshly derived alveolar macrophages. *In Vitro Cell Dev. Biol. Anim.* **25**:44–48 (1989).
29. J. A. Steinkamp, J. S. Wilson, G. C. Saunders, and C. C. Stewart. Phagocytosis—flow cytometric quantitation with fluorescent microspheres. *Science.* **215**:64–66 (1982).
30. F. Schroeder, and D. A. Kinden. Measurement of phagocytosis using fluorescent latex beads. *J. Biochem. Biophys. Methods.* **8**:15–27 (1983).
31. A. Palecanda, J. Paulauskis, E. Al-Mutairi, A. Imrich, G. Z. Qin, H. Suzuki, T. Kodama, K. Tryggvason, H. Koziel, and L. Kobzik. Role of the scavenger receptor MARCO in alveolar macrophage binding of unopsonized environmental particles. *J. Exp. Med.* **189**:1497–1506 (1999).
32. G. J. Dougherty, and W. H. McBride. Macrophage Heterogeneity. *J. Clin. Lab. Immun.* **14**:1–11 (1984).
33. I. Carr. *The Macrophage: A Review of Ultrastructure and Function.* Academic Press, London, 1973.
34. D. Cox, P. Chang, Q. Zhang, P. G. Reddy, G. M. Bokoch, and S. Greenberg. Requirements for both Rac1 and Cdc42 in membrane ruffling and phagocytosis in leukocytes. *J. Exp. Med.* **186**:1487–1494 (1997).
35. M. M. Myat, S. Anderson, L. A. H. Allen, and A. Aderem. MARCKS regulates membrane ruffling and cell spreading. *Curr. Biol.* **7**:611–614 (1997).
36. J. Israelchvili. *Intermolecular and Surface Forces.* Academic Press, San Diego, 1992.
37. E. M. V. Hoek, and G. K. Agarwal. Extended DLVO interactions between spherical particles and rough surfaces. *J. Colloid Interface Sci.* **298**:50–58 (2006).
38. W. J. Kowalski, W. P. Bahnfleth, and T. S. Whittam. Filtration of airborne microorganisms: modeling and prediction. *ASHRAE Trans.* **105**:4–17 (1999).
39. G. W. Burnett, and G. S. Schuster. Pathogenic microbiology. The C.V. Mosby Co., St. Louis, 1973.